I&EC research
Industrial & Engineering Chemistry Research

Article

pubs.acs.org/IECR

Enhanced Activity of Ti-Modified V_2O_5/CeO_2 Catalyst for the Selective Catalytic Reduction of NO_x with NH_3

Zhihua Lian, Fudong Liu,* and Hong He*

State Key Joint Laboratory of Environment Simulation and Pollution Control, Research Center for Eco-Environmental Sciences, Chinese Academy of Sciences, Beijing 100085, PR China

Supporting Information

ABSTRACT: A novel $V_2O_5/CeTiO_x$ catalyst showed excellent catalytic performance in the selective catalytic reduction (SCR) of NO_x with NH_3. The addition of Ti into V_2O_5/CeO_2 enhanced catalytic activity, N_2 selectivity, and resistance against SO_2 and H_2O. These catalysts were also characterized by N_2 adsorption, XRD, XPS, and H_2-TPR. The lower crystallinity, more reduced species, better dispersion of surface vanadium species, and more acid sites due to the modification of V_2O_5/CeO_2 with TiO_2 all improved the NH_3−SCR activity significantly. Based on *in situ* DRIFTS, it was concluded that the NH_3−SCR reaction over $V_2O_5/CeTiO_x$ and V_2O_5/CeO_2 mainly followed the Eley−Rideal mechanism.

1. INTRODUCTION

Nitrogen oxides (NO, NO_2, N_2O), emitted from automobile exhaust gas and industrial combustion of fossil fuels, have been a major source of air pollution, causing a variety of environmentally harmful effects such as photochemical smog, acid rain, and haze formation.[1,2] Selective catalytic reduction of NO_x with NH_3 (NH_3−SCR) has been used extensively for NO_x abatement, and the most widely used catalyst system is V_2O_5−$WO_3(MoO_3)/TiO_2$.[3−5] However, there are still some problems with the application of this system, such as a narrow operating temperature window of 300−400 °C and low N_2 selectivity in the high temperature range,[4,6] which greatly restrict its further application in the deNO_x process for mobile sources. Accordingly, the in-depth study and improvement of vanadium-based catalysts for NH_3−SCR is still of great importance in the field of environmental catalysis.[3,6−11]

Recently, ceria-based catalysts, such as Ce−Ti oxides[12−14] and CeO_2−WO_3,[15,16] have attracted intensive interest for SCR reaction studies due to the high oxygen storage capacity and excellent redox properties of ceria.[17,18] A previous study by Li et al.[19] showed that V_2O_5/CeO_2 catalysts exhibited high NH_3−SCR activity, and the NO conversion increased significantly with the increase of V_2O_5 loading. It was reported that the $V_{0.75}Ce$ oxide catalyst exhibited higher NH_3−SCR activity than the conventional V_2O_5−WO_3/TiO_2 catalyst below 350 °C.[20] TiO_2 is often used as favorable support material for NO abatement, and the catalyst could show good low-temperature catalytic activity and excellent SO_2 durability, because TiO_2 essentially does not react with either SO_3 or SO_2 above 200 °C.[21,22] In the present study, the addition of Ti enhanced NH_3−SCR activity remarkably, and stronger resistance against SO_2 was simultaneously obtained over $V_2O_5/CeTiO_x$. At the same time, the $V_2O_5/CeTiO_x$ catalysts are low-cost compared with V_2O_5/CeO_2 catalysts, due to the Ti precursor ($Ti(SO_4)_2$) being much cheaper than the Ce precursor ($Ce(NO_3)_3{\cdot}6H_2O$).

2. EXPERIMENTAL METHODS

2.1. Catalyst Synthesis and Catalytic Performance.

CeO_2 and $CeTiO_x$ were prepared by a homogeneous precipitation method using $Ce(NO_3)_3{\cdot}6H_2O$ and $Ti(SO_4)_2$ as precursors and urea as a precipitator. The mole ratio of Ce and Ti in $CeTiO_x$ was 1:1. The mixed solution was heated to 90 °C and held there for 12 h under vigorous stirring. After filtration and washing with deionized water, the resulting precipitate was dried at 100 °C overnight and subsequently calcined at 500 °C for 3 h. Then, the 3 wt % V_2O_5/CeO_2 and 3 wt % $V_2O_5/CeTiO_x$ catalysts were prepared by the impregnation method using a NH_4VO_3 precursor. After impregnation, the excess water was removed in a rotary evaporator at 60 °C. The sample was first dried at 100 °C overnight followed by calcination at 500 °C for 3 h.

The SCR activity tests were carried out in a fixed-bed quartz flow reactor with the following reaction conditions: 500 ppm of NO, 500 ppm of NH_3, 5% O_2, 5% H_2O (when used), 100 ppm of SO_2 (when used), balanced N_2, and GHSV = 50 000 h^{-1}. The effluent gas, including NO, NH_3, NO_2, and N_2O, was continuously analyzed by an online NEXUS 670-FTIR spectrometer equipped with a gas cell with 0.2 dm^3 volume. The FTIR spectra were collected after 1 h when the SCR reaction reached a steady state, and the NO_x conversion and N_2 selectivity were calculated as follows:

$$NO_x\ \text{conversion} = \left(1 - \frac{[NO]_{out} + [NO_2]_{out}}{[NO]_{in} + [NO_2]_{in}}\right) \times 100\%$$

Received: October 23, 2014
Revised: November 20, 2014
Accepted: November 24, 2014
Published: November 24, 2014

dx.doi.org/10.1021/ie504188s | *Ind. Eng. Chem. Res.* 2014, 53, 19506−19511

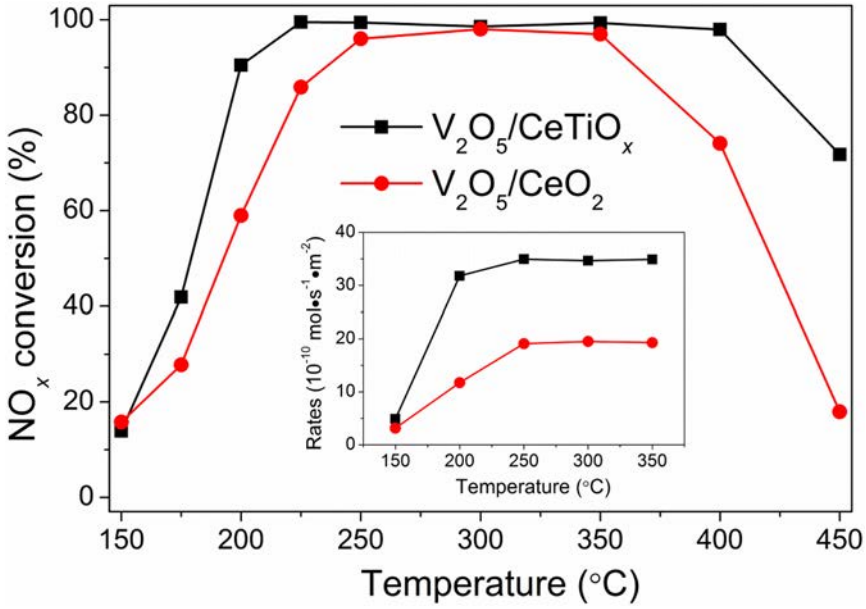

Figure 1. NH_3−SCR activities and reaction rates normalized by surface area of $V_2O_5/CeTiO_x$ and V_2O_5/CeO_2 catalysts. Reaction conditions: [NO] = [NH_3] = 500 ppm, [O_2] = 5 vol %, N_2 balance, total flow rate 500 mL/min, and GHSV = 50 000 h^{-1}.

$$N_2 \text{ selectivity} = \frac{[NO]_{in} + [NH_3]_{in} - [NO_2]_{out} - 2[N_2O]_{out}}{[NO]_{in} + [NH_3]_{in}} \times 100\%$$

2.2. Catalyst Characterization. The surface area and pore characterization of the catalysts were obtained from N_2 adsorption/desorption analysis at −196 °C using a Quantachrome Quadrasorb SI-MP. Prior to the N_2 physisorption, the catalysts were degassed at 300 °C for 5 h. Surface areas were determined using the BET equation in the 0.05−0.35 partial pressure range. Pore volumes and average pore diameters were determined by the Barrett−Joyner−Halenda (BJH) method from the desorption branches of the isotherms.

Powder X-ray diffraction (XRD) measurements of the catalysts were carried out on a computerized PANalytical X'Pert Pro diffractometer with Cu Kα (λ = 0.15406 nm) radiation. The data were collected for 2θ from 10 to 80° at 8°/min with the step size of 0.07°.

The H_2-TPR experiments were carried out on a Micromeritics AutoChem 2920 chemisorption analyzer. The samples (50 mg) were placed in a quartz reactor and pretreated at 300 °C in a flow of 20 vol % O_2/Ar (50 mL/min) for 0.5 h and cooled down to room temperature (30 °C) followed by Ar purging for 0.5 h. Then a 50 mL/min gas flow of 10% H_2 in Ar was passed over the samples through a cold trap to the detector. The reduction temperature was linearly raised at 10 °C min^{-1} from 30 to 1000 °C.

X-ray photoelectron spectroscopy (XPS) results of the catalysts were recorded on a scanning X-ray microprobe (Axis Ultra, Kratos Analytical Ltd.) using Al Kα radiation (1486.7 eV). All the binding energies were calibrated using the C 1s peak (BE = 284.8 eV) as a standard.

The *in situ* DRIFTS experiments were performed on an FTIR spectrometer (ThermoFisher, Nicolet Nexus 670) equipped with a smart collector and an MCT/A detector cooled by liquid nitrogen. The reaction temperature was controlled precisely by an Omega programmable temperature controller. Prior to each experiment, the sample was pretreated at 400 °C for 0.5 h in a flow of 20 vol % O_2/N_2 and then cooled down to 175 °C. The background spectra were collected in flowing N_2 and automatically subtracted from the sample spectrum. The reaction conditions were controlled as follows: 300 mL/min total flow rate, 500 ppm of NH_3 or/and 500 ppm of NO + 5 vol % O_2, and N_2 balance. All spectra were recorded by accumulating 100 scans with a resolution of 4 cm^{-1}.

3. RESULTS AND DISCUSSION

3.1. SCR Activity Tests. Figure 1 shows the NH_3−SCR activities and reaction rates normalized by surface area over $V_2O_5/CeTiO_x$ and V_2O_5/CeO_2 catalysts. The V_2O_5/CeO_2 catalyst exhibited nearly 100% NO_x conversion in the temperature window of 250−350 °C. Clearly, the $V_2O_5/CeTiO_x$ catalyst showed higher catalytic activity than V_2O_5/CeO_2 not only in the low temperature range but also in the high temperature range. The modification of TiO_2 broadened the operating temperature window remarkably, and the NO_x conversion in the temperature window of 200−400 °C was higher than 90%. Both the catalysts showed high N_2 selectivity (as shown in Figure S1). N_2 selectivity over the $V_2O_5/CeTiO_x$ catalyst was a little higher than that over V_2O_5/CeO_2. At 450 °C, 92% and 84% N_2 selectivity were obtained over $V_2O_5/CeTiO_x$ and V_2O_5/CeO_2, respectively. The lower N_2 selectivity over V_2O_5/CeO_2 was due to the formation of NO_2 and N_2O and 105 ppm of NO_2 and 25 ppm of N_2O were produced at 450 °C. The NH_3−SCR reaction rates normalized by surface area over the $V_2O_5/CeTiO_x$ catalyst were also much higher than those over the V_2O_5/CeO_2 catalyst higher than 150 °C. The modification by TiO_2 enhanced significantly the NH_3−SCR activity and reaction rate normalized by surface area over the $V_2O_5/CeTiO_x$ catalyst.

In practical use, the SCR reaction atmosphere usually contains some fraction of H_2O and SO_2. Therefore, the effect of 5% H_2O and 100 ppm of SO_2 separately on the SCR reaction over $V_2O_5/CeTiO_x$ and V_2O_5/CeO_2 catalysts was investigated. As shown in Figure 2, after H_2O was introduced at

dx.doi.org/10.1021/ie504188s | *Ind. Eng. Chem. Res.* 2014, 53, 19506−19511

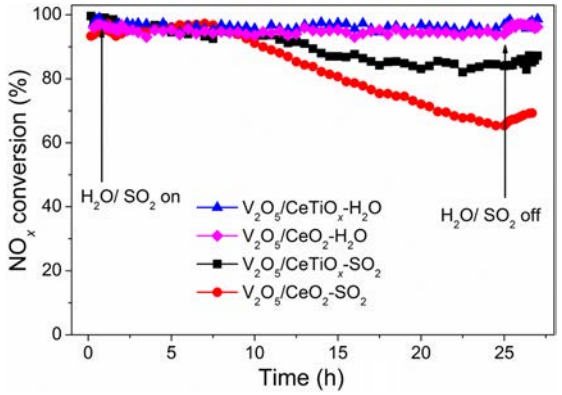

Figure 2. Effect of 5% H_2O and 100 ppm of SO_2 separately on catalytic performance over $V_2O_5/CeTiO_x$ and V_2O_5/CeO_2 catalysts at 250 °C. Reaction conditions: [NO] = [NH_3] = 500 ppm, [O_2] = 5 vol %, [H_2O] = 5 vol % (when used), [SO_2] = 100 ppm (when used), N_2 balance, total flow rate 500 mL/min, and GHSV = 50 000 h^{-1}.

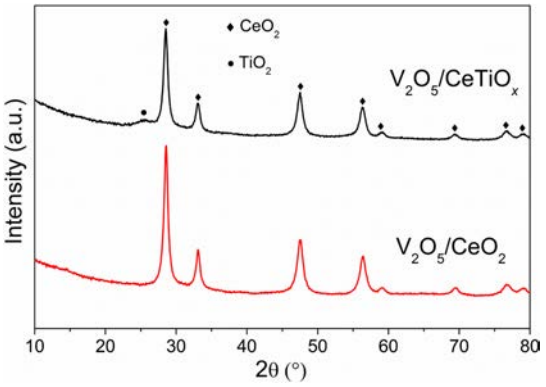

Figure 3. Powder XRD patterns of $V_2O_5/CeTiO_x$ and V_2O_5/CeO_2 catalysts.

250 °C, NO_x conversion over $V_2O_5/CeTiO_x$ and V_2O_5/CeO_2 catalysts did not decrease during the 24 h test and could be maintained at nearly 100%. These two catalysts showed good resistance to H_2O poisoning without apparent decline of SCR activity in long-term operation. The presence of SO_2 showed an obvious interference with the SCR activity over the V_2O_5/CeO_2 catalyst and the NO_x conversion decreased to lower than 60% after 24 h test. By contrast, the $V_2O_5/CeTiO_x$ catalyst exhibited stronger resistance against SO_2, and nearly 90% NO_x conversion was still obtained after a 24 h test. After SO_2 was cut off, the NH_3−SCR activities over both $V_2O_5/CeTiO_x$ and V_2O_5/CeO_2 catalysts could not be restored to the original level. The $V_2O_5/CeTiO_x$ catalyst exhibited strong resistance to H_2O and SO_2 poisoning.

The NH_3−SCR activity test results of $V_2O_5/CeTiO_x$ and V_2O_5/CeO_2 catalysts after 100 ppm of SO_2 poisoning for 24 h are shown in Figure S2. The catalytic activity of the catalysts after sulfation was lower than that of fresh catalysts in the range 150−300 °C. NO_x conversion decreased from 100% to 45% at 225 °C over $V_2O_5/CeTiO_x$. After sulfation, the $V_2O_5/CeTiO_x$ catalyst still showed a little higher NO_x conversion than V_2O_5/CeO_2. At 250 °C, 80% and 70% NO_x conversion was obtained over $V_2O_5/CeTiO_x$ and V_2O_5/CeO_2, respectively. This proved again that the $V_2O_5/CeTiO_x$ catalyst showed higher SO_2 resistance than V_2O_5/CeO_2.

3.2. N_2 Physisorption and XRD. The BET surface areas, pore volumes, and average pore diameters of $V_2O_5/CeTiO_x$ and V_2O_5/CeO_2 catalysts are shown in Table 1. The surface areas and pore volumes of $V_2O_5/CeTiO_x$ catalysts were much lower than those of V_2O_5/CeO_2. The pore diameter of these catalysts showed little difference. This indicated that the modification by TiO_2 reduced the surface area and pore volume of $V_2O_5/CeTiO_x$.

Powder XRD was used to investigate the crystal structures of $V_2O_5/CeTiO_x$ and V_2O_5/CeO_2 catalysts. As shown in Figure 3, the main peaks in the diffraction profiles can be attributed to CeO_2 with the cubic fluorite structure (43−1002). The intensity of the peaks of the $V_2O_5/CeTiO_x$ catalyst weakened compared with that of the V_2O_5/CeO_2 catalyst, indicating that the modification by TiO_2 led to a decrease in CeO_2 crystallinity. The grain size of CeO_2 over the $V_2O_5/CeTiO_x$ catalyst (13.0 nm) was lower than that over V_2O_5/CeO_2 (13.6 nm). The broad diffraction peak at 25° appearing in the XRD pattern of $V_2O_5/CeTiO_x$ was assigned to anatase TiO_2 (21−1272). No vanadium species such as V_2O_5 and $CeVO_4$ were detected, suggesting that vanadium species were highly dispersed on these catalysts. The addition of Ti affected the structure of the catalyst. It weakened the crystallinity and reduced the grain size.

3.4. XPS Analysis. Table 1 also illustrates the surface atomic concentration on the $V_2O_5/CeTiO_x$ and V_2O_5/CeO_2 catalysts. The surface Ti concentration was much lower than the surface Ce concentration, indicating that Ti mainly existed in the bulk phase of the $V_2O_5/CeTiO_x$ catalysts. The surface vanadium concentration on $V_2O_5/CeTiO_x$ catalysts was higher than that on V_2O_5/CeO_2 catalysts. The addition of titanium improved the dispersion of surface vanadium species on $V_2O_5/CeTiO_x$ catalysts, and higher surface vanadium concentration was obtained, which could contribute to the enhancement of catalytic performance.

Furthermore, the higher surface concentration of vanadium species on the $V_2O_5/CeTiO_x$ catalyst surface could also enhance SO_2 resistance. Although V_2O_5 should be tolerable for SO_2, there were still Ti and Ce components in $V_2O_5/CeTiO_x$ catalysts. $Ti(SO_4)_2$ and $TiOSO_4$ could decompose above 300 °C. SO_2 could have serious impacts on CeO_2 and TiO_2 at 250 °C. Therefore, the catalytic activity over $V_2O_5/CeTiO_x$ decreased at some degree after a 24 h SO_2 test.

Figure 4 shows the fitted O 1s peaks of $V_2O_5/CeTiO_x$ and V_2O_5/CeO_2 catalysts. The XPS of O 1s were deconvoluted into three peaks. The peaks at 529.2−529.6 eV could be attributed to lattice oxygen O^{2-} (denoted as O_β). The peaks at 530.9−531.2 eV and 532.3−532.6 eV were assigned to surface adsorbed oxygen (denoted as O_α) and chemisorbed water

Table 1. Structural Parameters and Surface Atomic Concentration of $V_2O_5/CeTiO_x$ and V_2O_5/CeO_2 Catalysts

				surface atomic concentration (%)			
catalysts	BET surface area (m^2/g)	pore volume (cm^3/g)	pore diameter (nm)	V	Ce	Ti	O
$V_2O_5/CeTiO_x$	59.61	0.0773	5.187	2.39	22.75	4.30	70.56
V_2O_5/CeO_2	91.90	0.1185	5.157	1.90	29.10		69.00

dx.doi.org/10.1021/ie504188s | Ind. Eng. Chem. Res. 2014, 53, 19506−19511

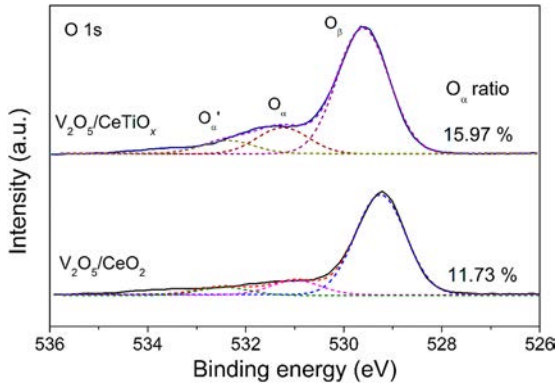

Figure 4. XPS results of O 1s on $V_2O_5/CeTiO_x$ and V_2O_5/CeO_2 catalysts.

(denoted as O_α'), respectively.[12,25] Usually, the surface oxygen O_α is more reactive in oxidation reactions due to its higher mobility than lattice oxygen O_β.[26] The relative concentration ratios of $O_\alpha/(O_\alpha+O_\beta+O_\alpha')$ were calculated and are listed on the right side of Figure 4. The $O_\alpha/(O_\alpha+O_\beta+O_\alpha')$ on the $V_2O_5/CeTiO_x$ catalyst was 15.97%, much higher than that on the V_2O_5/CeO_2 catalyst, indicating the presence of more abundant surface oxygen. However, NO oxidation activity over the $V_2O_5/CeTiO_x$ catalyst was lower (Figure S3), which meant that some other changes such as acid sites induced by Ti addition inhibited the oxidation of NO.

3.3. H_2-TPR. Figure 5 reveals the H_2-TPR profiles of the $V_2O_5/CeTiO_x$ and V_2O_5/CeO_2 catalysts. $V_2O_5/CeTiO_x$ shows

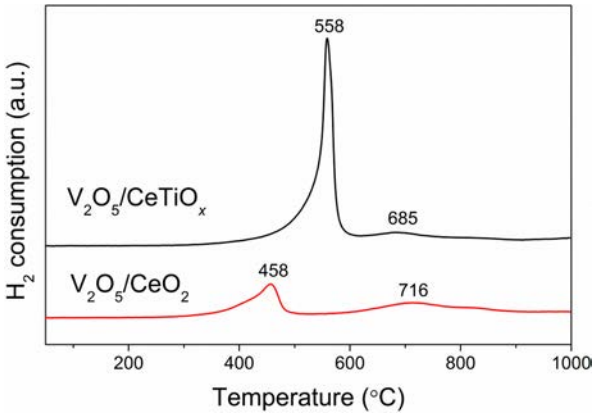

Figure 5. H_2-TPR results of $V_2O_5/CeTiO_x$ and V_2O_5/CeO_2 catalysts.

two H_2 consumption peaks centered at about 558 and 685 °C, while they appear at about 458 and 716 °C for V_2O_5/CeO_2. According to the literature,[10,23,24] the low temperature peaks between 400 and 600 °C and high temperature peaks between 600 and 800 °C can be assigned to the reduction of surface oxygen and lattice oxygen, respectively. The H_2 reduction temperature over V_2O_5/CeO_2 catalyst was lower than that over $V_2O_5/CeTiO_x$, which is in good agreement with the NO oxidation activity (Figure S3). However, the amount of H_2 consumed over $V_2O_5/CeTiO_x$ was significantly larger than that over V_2O_5/CeO_2. This suggested that an interaction did exist between Ce and Ti and the presence of Ti ions weakened the Ce−O bond in $V_2O_5/CeTiO_x$, which made the Ce−O component easily reducible. It indicated that the modification of TiO_2 resulted in better dispersion and more reduced species. The smaller amount of H_2 consumption over V_2O_5/CeO_2 indicated less reduced species and could lead to a lower O_α ratio.

3.5. *In Situ* DRIFTS Results. To investigate the surface acid properties of the catalysts, the *in situ* DRIFTS of NH_3 adsorption on $V_2O_5/CeTiO_x$ and V_2O_5/CeO_2 catalysts at 175 °C were recorded, with the results shown in Figure 6A. The

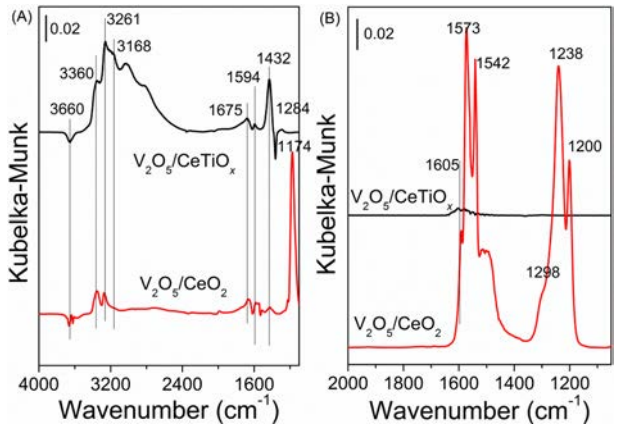

Figure 6. *In situ* DRIFTS of NH_3 adsorption (A) and NO_x adsorption (B) of $V_2O_5/CeTiO_x$ and V_2O_5/CeO_2 catalysts at 175 °C.

bands at 1594 and 1174 and at 1284 cm^{-1} were assigned to asymmetric and symmetric bending vibrations of the N−H bonds in NH_3 coordinately linked to Lewis acid sites, and the bands at 1432 and 1681 cm^{-1} were attributed to asymmetric and symmetric bending vibrations of NH_4^+ species on Brønsted acid sites.[25,27,28] In the NH stretching vibration region of coordinated NH_3, bands were found at 3360, 3261, and 3168 cm^{-1}.[29] Some negative bands around 3660 cm^{-1} were also found, which could be assigned to surface O−H stretching.[28] Although the BET specific area of $V_2O_5/CeTiO_x$ (59.61 m^2/g) was much lower than that of V_2O_5/CeO_2 (91.90 m^2/g), the intensity of bands attributed to NH_3 adsorption on the former was much higher than that of the latter, indicating that more acid sites existed on the $V_2O_5/CeTiO_x$ surface. The modification of TiO_2 led to better dispersion of surface vanadium species, and more acid sites were obtained. More acid sites could facilitate the adsorption of NH_3 and participate in the SCR reaction, leading to better catalytic activity. Figure 6B shows the DRIFT spectra of NO + O_2 adsorption on $V_2O_5/CeTiO_x$ and V_2O_5/CeO_2 catalysts at 175 °C. When the catalysts were exposed to NO + O_2, several bands assigned to nitrate species were observed, including monodentate nitrate (1298, 1542 cm^{-1}), bridging nitrate (1200, 1605 cm^{-1}), and bidentate nitrate (1238, 1573 cm^{-1}).[30−32] Due to its more abundant acid sites, the $V_2O_5/CeTiO_x$ catalysts showed a smaller amount of adsorbed NO_x species than V_2O_5/CeO_2.

To investigate the reactivity of adsorbed NH_3 species in the SCR reaction on the $V_2O_5/CeTiO_x$ and V_2O_5/CeO_2 catalysts, the *in situ* DRIFTS of reaction between preadsorbed NH_3 and NO + O_2 at 175 °C were recorded as a function of time (Figure 7A and B). After exposure to NH_3, the $V_2O_5/CeTiO_x$ and V_2O_5/CeO_2 catalyst surfaces were covered by several NH_3 species, but when NO + O_2 was introduced, the bands due to adsorbed NH_3 species diminished and were replaced by surface nitrate species. This indicates that both the coordinated NH_3 bound to Lewis acid sites and NH_4^+ bound to Brønsted acid sites can participate in the NH_3−SCR reaction.

dx.doi.org/10.1021/ie504188s | *Ind. Eng. Chem. Res.* 2014, 53, 19506−19511

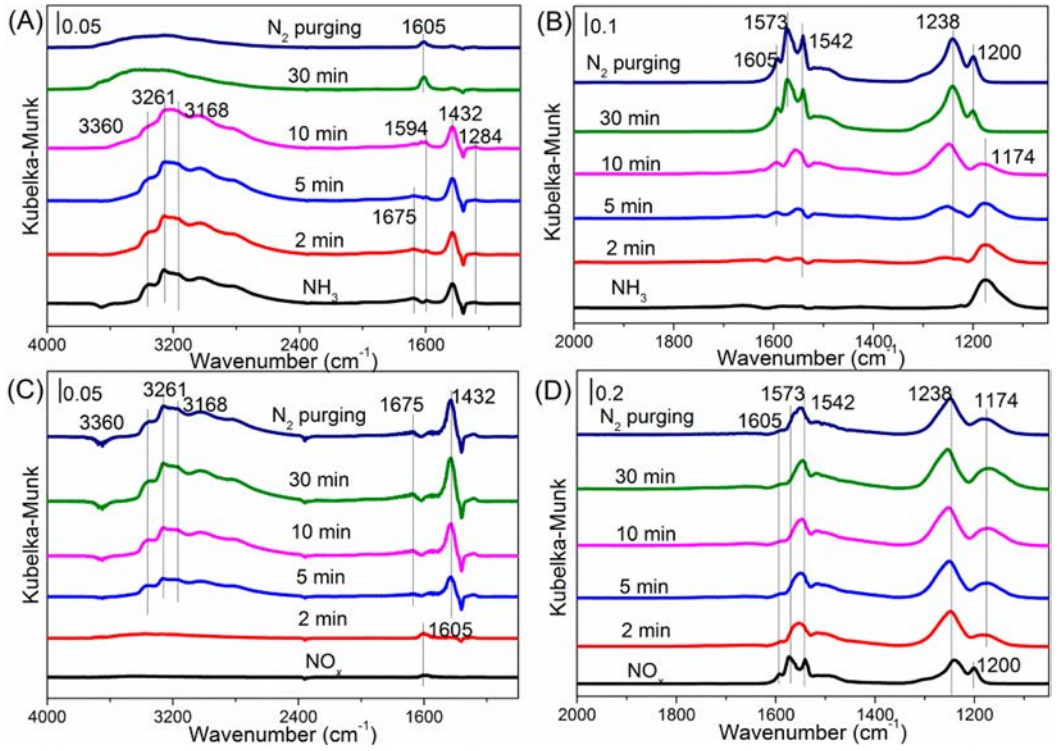

Figure 7. *In situ* DRIFTS of NO + O_2 reacted with preadsorbed NH_3 species on $V_2O_5/CeTiO_x$ (A) and V_2O_5/CeO_2 (B), NH_3 reacted with preadsorbed NO_x species on $V_2O_5/CeTiO_x$ (C) and V_2O_5/CeO_2 (D) at 175 °C.

In situ DRIFTS of reaction between preadsorbed NO_x and NH_3 at 175 °C are shown in Figure 7C and D. When NH_3 was introduced, the bands attributed to nitrate species on $V_2O_5/CeTiO_x$ diminished and NH_3 adsorption species appeared. Compared to the amount of adsorbed NO_x species on $V_2O_5/CeTiO_x$, the amount on V_2O_5/CeO_2 was much larger. However, most of the bands ascribed to nitrate on V_2O_5/CeO_2 stayed unchanged when NH_3 was introduced, indicating that the adsorbed nitrate was almost inactive. The NH_3–SCR reaction over V_2O_5/CeO_2 mainly followed the Eley–Rideal mechanism, in which gaseous NO reacts with adsorbed NH_3 species to finally form N_2 and H_2O. The modification by Ti enhanced the acidity, which could favor the SCR reaction. The formation of surface nitrate was inhibited, and only a small amount of nitrate was formed. Therefore, the NH_3–SCR reaction over $V_2O_5/CeTiO_x$ also mainly followed the Eley–Rideal scheme.

4. CONCLUSIONS

$V_2O_5/CeTiO_x$ showed higher NH_3–SCR activity over a broad temperature window and stronger resistance against SO_2 and H_2O than V_2O_5/CeO_2. The modification by Ti resulted in lower crystallinity, more reduced species, better dispersion of surface vanadium species, and higher acidity, which were all responsible for the excellent NH_3–SCR performance obtained over the $V_2O_5/CeTiO_x$ catalyst. The NH_3–SCR reaction over $V_2O_5/CeTiO_x$ and V_2O_5/CeO_2 mainly followed the Eley–Rideal mechanism.

■ ASSOCIATED CONTENT

Supporting Information

N_2 selectivity of $V_2O_5/CeTiO_x$ and V_2O_5/CeO_2 catalysts, NH_3–SCR activity of the catalysts after sulfation, and NO and NH_3 separate oxidation activity. This material is available free of charge via the Internet at http://pubs.acs.org.

■ AUTHOR INFORMATION

Corresponding Authors

*Tel.: +86 10 62849123. Fax: +86 10 62849123. E-mail: fdliu@rcees.ac.cn (F.L.).

*Tel.: +86 10 62849123. Fax: +86 10 62849123. E-mail: honghe@rcees.ac.cn (H.H.).

Notes

The authors declare no competing financial interest.

■ ACKNOWLEDGMENTS

This study was financially supported by the National Natural Science Foundation of China (51108446, 51221892) and the Ministry of Science and Technology, China (2012AA062506).

■ REFERENCES

(1) Qi, G. S.; Yang, R. T.; Chang, R. MnO_x-CeO_2 mixed oxides prepared by co-precipitation for selective catalytic reduction of NO with NH_3 at low temperatures. *Appl. Catal., B* **2004**, *51*, 93.

(2) Bosch, H.; Janssen, F. Formation and control of nitrogen oxides. *Catal. Today* **1988**, *2*, 369.

(3) Huang, Z. G.; Zhu, Z. P.; Liu, Z. Y.; Liu, Q. Y. Formation and reaction of ammonium sulfate salts on V_2O_5/AC catalyst during selective catalytic reduction of nitric oxide by ammonia at low temperatures. *J. Catal.* **2003**, *214*, 213.

(4) Busca, G.; Lietti, L.; Ramis, G.; Berti, F. Chemical and mechanistic aspects of the selective catalytic reduction of NO_x by ammonia over oxide catalysts: A review. *Appl. Catal., B* **1998**, *18*, 1.

(5) Busca, G.; Larrubia, M. A.; Arrighi, L.; Ramis, G. Catalytic abatement of NO_x: Chemical and mechanistic aspects. *Catal. Today.* **2005**, *107–108*, 139.

(6) Casanova, M.; Schermanz, K.; Llorca, J.; Trovarelli, A. Improved high temperature stability of NH_3-SCR catalysts based on rare earth

vanadates supported on TiO_2-WO_3-SiO_2. *Catal. Today.* **2012**, *184*, 227.
(7) Krocher, O.; Elsener, M. Chemical deactivation of V_2O_5/WO_3-TiO_2 SCR catalysts by additives and impurities from fuels, lubrication oils, and urea solution - I. Catalytic studies. *Appl. Catal., B* **2008**, *77*, 215.
(8) Kristensen, S. B.; Kunov-Kruse, A. J.; Riisager, A.; Rasmussen, S. B.; Fehrmann, R. High performance vanadia−anatase nanoparticle catalysts for the Selective Catalytic Reduction of NO by ammonia. *J. Catal.* **2011**, *284*, 60.
(9) Klimczak, M.; Kern, P.; Heinzelmann, T.; Lucas, M.; Claus, P. High-throughput study of the effects of inorganic additives and poisons on NH_3-SCR catalysts Part I: V_2O_5-WO_3/TiO_2 catalysts. *Appl. Catal., B* **2010**, *95*, 39.
(10) Chen, L.; Li, J. H.; Ge, M. F. Promotional Effect of Ce-doped V_2O_5-WO_3/TiO_2 with Low Vanadium Loadings for Selective Catalytic Reduction of NO_x by NH_3. *J. Phys. Chem. C* **2009**, *113*, 21177.
(11) Kobayashi, M.; Kuma, R.; Masaki, S.; Sugishima, N. TiO_2-SiO_2 and V_2O_5/TiO_2-SiO_2 catalyst: Physico-chemical characteristics and catalytic behavior in selective catalytic reduction of NO by NH_3. *Appl. Catal., B* **2005**, *60*, 173.
(12) Shan, W.; Liu, F.; He, H.; Shi, X.; Zhang, C. An environmentally-benign CeO_2-TiO_2 catalyst for the selective catalytic reduction of NO_x with NH_3 in simulated diesel exhaust. *Catal. Today.* **2012**, *184*, 160.
(13) Li, P.; Xin, Y.; Li, Q.; Wang, Z. P.; Zhang, Z. L.; Zheng, L. R. Ce-Ti Amorphous Oxides for Selective Catalytic Reduction of NO with NH_3: Confirmation of Ce-O-Ti Active Sites. *Environ. Sci. Technol.* **2012**, *46*, 9600.
(14) Xu, W.; Yu, Y.; Zhang, C.; He, H. Selective catalytic reduction of NO by NH_3 over a Ce/TiO_2 catalyst. *Catal. Commun.* **2008**, *9*, 1453.
(15) Chen, L.; Li, J.; Ablikim, W.; Wang, J.; Chang, H.; Ma, L.; Xu, J.; Ge, M.; Arandiyan, H. CeO_2-WO_3 Mixed Oxides for the Selective Catalytic Reduction of NO_x by NH_3 Over a Wide Temperature Range. *Catal. Lett.* **2011**, *141*, 1859.
(16) Shan, W.; Liu, F.; He, H.; Shi, X.; Zhang, C. Novel cerium-tungsten mixed oxide catalyst for the selective catalytic reduction of NO_x with NH_3. *Chem. Commun.* **2011**, *47*, 8046.
(17) Qi, G.; Yang, R. T. A superior catalyst for low-temperature NO reduction with NH_3. *Chem. Commun.* **2003**, 848.
(18) Qi, G. S.; Yang, R. T. Performance and kinetics study for low-temperature SCR of NO with NH_3 over MnO_x-CeO_2 catalyst. *J. Catal.* **2003**, *217*, 434.
(19) Li, C.; Li, Q.; Lu, P.; Cui, H.; Zeng, G. Characterization and performance of V_2O_5/CeO_2 for NH_3-SCR of NO at low temperatures. *Front. Environ. Sci. Eng.* **2012**, *6*, 156.
(20) Peng, Y.; Wang, C.; Li, J. Structure-activity relationship of VO_x/CeO_2 nanorod for NO removal with ammonia. *Appl. Catal., B* **2014**, *144*, 538.
(21) F, N.; I, H. The state-of-the-art technology of NO_x control. *Catal. Today* **1996**, *29*, 109.
(22) Ye, D.; Tian, L.; Hong, L. Effect of TiO_2 surface properties on the SCR activity of NO_x emission abatement catalysis. *J. Environ. Sci. (Beijing, China)* **2002**, *14*, 530.
(23) Trovarelli, A.; Dolcetti, G.; de Leitenburg, C.; Kaspar, J.; Finetti, P.; Santoni, A. Rh-CeO_2 interaction induced by high-temperature reduction. Characterization and catalytic behaviour in transient and continuous conditions. *J. Chemi. Soc., Faraday Trans.* **1992**, *88*, 1311.
(24) Reiche, M. A.; Baiker, A. Vanadia grafted on TiO_2-SiO_2, TiO_2 and SiO_2 aerogels Structural properties and catalytic behaviour in selective reduction of NO by NH_3. *Appl. Catal., B* **1999**, *23*, 187.
(25) Gu, T.; Jin, R.; Liu, Y.; Liu, H.; Weng, X.; Wu, Z. Promoting effect of calcium doping on the performances of MnO_x/TiO_2 catalysts for NO reduction with NH_3 at low temperature. *Appl. Catal., B* **2013**, *129*, 30.
(26) Wu, Z. B.; Jin, R. B.; Liu, Y.; Wang, H. Q. Ceria modified MnO_x/TiO_2 as a superior catalyst for NO reduction with NH_3 at low-temperature. *Catal. Commun.* **2008**, *9*, 2217.
(27) Yang, S. J.; Wang, C. Z.; Li, J. H.; Yan, N. Q.; Ma, L.; Chang, H. Z. Low temperature selective catalytic reduction of NO with NH_3 over Mn-Fe spinel: Performance, mechanism and kinetic study. *Appl. Catal., B* **2011**, *110*, 71.
(28) Wu, Z. B.; Jiang, B. Q.; Liu, Y.; Wang, H. Q.; Jin, R. B. DRIFT study of manganese/titania-based catalysts for low-temperature selective catalytic reduction of NO with NH_3. *Environ. Sci. Technol.* **2007**, *41*, 5812.
(29) Topsoe, N. Y. Mechanism of the selective catalytic reduction of nitric oxide by ammonia elucidated by in situ online Fourier Transform Infrared spectroscopy. *Science* **1994**, *265*, 1217.
(30) Gao, R.; Zhang, D.; Liu, X.; Shi, L.; Maitarad, P.; Li, H.; Zhang, J.; Cao, W. Enhanced catalytic performance of V_2O_5−$WO_3/Fe_2O_3/TiO_2$ microspheres for selective catalytic reduction of NO by NH_3. *Catal. Sci. Technol.* **2013**, *3*, 191.
(31) Hadjiivanov, K. I. Identification of Neutral and Charged N_xO_y Surface Species by IR Spectroscopy. *Catal. Rev. Sci. Eng.* **2000**, *42*, 71.
(32) Liu, C.; Chen, L.; Li, J.; Ma, L.; Arandiyan, H.; Du, Y.; Xu, J.; Hao, J. Enhancement of Activity and Sulfur Resistance of CeO_2 Supported on TiO_2-SiO_2 for the Selective Catalytic Reduction of NO by NH_3. *Environ. Sci. Technol.* **2012**, *46*, 6182.